Scientific Reports

https://doi.org/10.1038/s41598-026-45350-2

Article in Press

Co-pyrolysis of agricultural biomass for potentially functional biochar: combined influence of both feedstocks and structural characterization

Received: 23 October 2025

Accepted: 18 March 2026

Published online: 27 March 2026

Cite this article as: Demir Z. & Bozkurt P.A. Co-pyrolysis of agricultural biomass for potentially functional biochar: combined influence of both feedstocks and structural characterization. *Sci Rep* (2026). https://doi.org/10.1038/s41598-026-45350-2

Zeynep Demir & Pınar Acar Bozkurt

Co-Pyrolysis of Agricultural Biomass for Potentially Functional Biochar: Combined influence of both Feedstocks and Structural Characterization

Zeynep Demir [1,*], Pınar Acar Bozkurt[2]

[1]Soil Fertilizer and Water Resources Central Research Institute, Ankara 06170, Türkiye

[2]Ankara University, Faculty of Science, Department of Chemistry, Ankara 06100, Türkiye

[*]Corresponding author: zdemir06@yahoo.com, ORCID: 0000 0002 7589 3216

Mobile: +90505 2914548. Office phone: +90312 315 65 60-64 / 218. Fax: +903123152931

Abstract

This study evaluates how the co-pyrolysis of two agricultural residues, corn stalk and rice husk, influences the physicochemical characteristics of the resulting biochar. Biochars were produced at 400 °C from each feedstock and from a 1:1 (w/w) mixture to assess interaction-driven behavior compared with the individual materials. The mixture biochar exhibited a broader particle-size distribution (SPAN=3.36±0.14) than the single-feedstock biochars, while maintaining a comparable BET surface area (13.17±0.42 $m^2 g^{-1}$) relative to rice husk biochar (13.90 ± 0.35 $m^2 g^{-1}$) and slightly higher than corn stalk biochar (11.96±0.28 $m^2 g^{-1}$). These results indicate that surface development was largely preserved despite particle coarsening, suggesting interaction effects between feedstocks rather than a purely additive mixing behavior. Zeta potential measurements showed negative surface charge for all samples (−25.7±1.3 to −33.7±1.2 mV), reflecting electrostatic surface characteristics associated with oxygen-containing functional groups and mineral phases, without being interpreted as direct evidence of adsorption performance. Mineral composition analysis revealed that the blended biochar integrated silica-rich and nutrient-associated inorganic phases, with Si, K, and Ca as major constituents. Spectroscopic and diffraction analyses further indicated a predominantly amorphous carbon matrix with retained mineral phases,

while microscopy confirmed heterogeneous morphology consistent with the combined contribution of both biomass sources. Overall, co-pyrolysis at 400 °C produced a biochar with integrated structural and chemical characteristics derived from both residues. These physicochemical properties suggest potential relevance for environmental applications such as soil amendment or contaminant management; however, application-based experiments (e.g., soil incubation, sorption, or column tests) are required to verify nutrient retention and adsorption performance under realistic conditions.

Keywords: Biochar, co-pyrolysis, agricultural biomass, interaction effects, structural characterization, surface functionality

1. Introduction

Demand for sustainable waste management and the use of environmentally friendly materials has led to increased research into agricultural biomass valorization. Pyrolysis has been identified as a promising thermochemical method to convert lignocellulosic waste into value added products (such as biochar)[1]. Biochar is a carbon rich by-product from pyrolysis of biomass that has many uses including soil amendment, water filtration, carbon sequestration and environmental remediation due to its porous nature, large surface area, and chemical properties[2,3].

Recent reviews have shown that the characteristics of biochar can be greatly affected by its feedstock and the conditions at which it is produced (i.e., pyrolysis conditions). They also pointed out that feedstock composition and pyrolysis conditions have direct impacts on biochar properties. As a result, it is essential to analyze and comprehend the structure-function relationship between biochar before and after production[1,4]. Research is beginning to show that the addition of another feedstock (i.e., co-feedstock) while producing biochar also creates interaction effects that will impact the physical and chemical properties of the resultant biochar[5,6]. Co-feeding two or more feedstocks, when

compared with using one feedstock, has been shown to create more pore space, increase surface reactivity and alter mineral composition due to the interaction of both organic and inorganic components during thermal conversion. However, further work is needed to understand exactly how these interaction effects and their associated structural properties of the resultant biochar are created when using mixed agricultural feedstock systems. Numerous studies have reported the use of co-pyrolysis for altering biochar yield and physicochemical properties by the interaction of blended feedstocks, and these alterations are very dependent on the blending ratio and temperature[7]. As it is suggested by recent research, performance-based claims (like adsorption in actual soils) can only be made based on the evidence of their application in practice since the characteristics used for characterization do not always correlate to those obtained from application in actual field situations[8].

More recently, research has been focusing on improving the use of carbon materials produced from biomass by combining various types of pyrolysis and co-pyrolysis methods with other complementary processing techniques. These types of processes may be physical or chemical activation, metal impregnation, hydrothermal carbonization or combined thermochemical treatments, and they can improve the surface area, pore structure, and reactivity of the resulting materials. For example, Petrović[9] found that hydrochar made from Fe-Mg modified materials has a much greater capacity for adsorbing lead ion than unmodified hydrochar. This case demonstrates the benefit of combining processes used to thermochemically convert biomass as well as methods of modifying biomass that improve the performance of carbon materials produced from biomass derived from biomass. This demonstrates that if you combine pyrolysis and other post-processes or activation processes, the result will be a greater number of active sites available for adsorption and/or catalysis. Furthermore, when you use co-pyrolysis techniques, the interaction between organic and inorganic components of the different types or sources of biomass during the thermal decomposition of biomass

affects some of the physicochemical properties of the resulting biochar produced from the biomass feedstock materials. The mechanism of how these interactions regarding pore formation, mineral distribution, and functionality on surfaces occurs is still poorly understood, as there may be many variables that influence these characteristics of feedstocks. However, it appears that they are generally affected by the type of feedstock used and the processing parameters used to fabricate the material[10].

Studies indicate that claims regarding performance (adsorption in actual soils) should be substantiated by field-based evidence derived from application methods. This is due to the fact that use of characterization metrics may not necessarily be indicative of field performance. Also, the increasing level of interest in systems based on biochar is substantiated by experimental evidence that biochar will enhance either the quality of soil or the performance of crops. For instance, Demir[11] suggested that biochar treatments led to a significant improvement in silage maize's physiological response when compared to using the standard drip irrigation technique. In another instance, the work of Demir and Bayraklı[12] showed that biochar amended soils were significantly improved (both chemically and physically) and that silage maize yields were increased, as was the water use efficiency and economic returns, under drought conditions. These findings demonstrate an example of providing performance-based evidence through actual field evidence of how biochar produced from agricultural biomass can improve the interaction between soil and plants under field conditions.

In this context, the present study aims to provide a comprehensive physicochemical and structural characterization of biochar produced from the co-pyrolysis of agricultural residues, with particular emphasis on understanding interaction effects between feedstocks through a multi-technique analytical approach. Although individual biomass-derived biochars such as those from corn stalk or rice husk have been widely studied[13,14] systematic investigations on their co-pyrolysis and the

resulting changes in morphology, crystallinity, elemental composition, and surface functionality remain limited. This study aims to address this gap by producing biochar from the co-pyrolysis of rice husk and corn stalk in a 1:1 (w/w) ratio at 400 °C and systematically investigating the interaction effects on its physicochemical properties. In this context, interaction effects were evaluated by comparing the properties of the co-pyrolyzed biochar with those of individual feedstock-derived biochars rather than assuming purely additive behavior. The findings provide new insights into how biomass mixing during pyrolysis influences the structural evolution of biochar. The integration of different analytical approaches provides a comprehensive understanding of the interaction effects induced by co-pyrolysis. This work contributes to the development of functional biochar materials by providing a detailed structure–property comparison.

2. Materials and method

2.1. Agricultural biomass and biochar production

In this study, agricultural biomass was selected as raw material for biochar production. Corn stalks were collected from an agricultural field in Konya Province, and rice husks were sourced from a rice cultivation area in Çorum Province, Türkiye. These feedstocks were used individually and in a 1:1 (w/w) mixture to prepare pyrolysis samples. Biochar was produced via slow pyrolysis at 400°C under oxygen-limited conditions. The obtained biochar material was subsequently sieved through a 0.25 mm mesh to ensure homogeneity and to prepare it for further physicochemical characterization. All pyrolysis and pre-treatment steps were conducted under controlled laboratory conditions. The pH and electrical conductivity (EC) of the biochar samples were determined in a biochar–water suspension at a ratio of 1:10 (w/v), following standard procedures[15,16]. The suspensions were equilibrated for 1 h under continuous stirring at room temperature, and measurements were performed using calibrated pH and EC meters. All pyrolysis experiments were conducted in independent batches under identical conditions, and representative biochar samples from each batch were subjected to physicochemical characterization to

ensure reproducibility. All physicochemical analyses were performed in triplicate (n = 3), and the results are reported as mean values. Where applicable, standard deviations were calculated and included to reflect experimental variability and improve the reliability of the comparisons.

2.2. Characterization techniques

The functional groups in the biochar were identified through Fourier Transform Infrared Spectroscopy (FT-IR) with a Perkin Elmer 400 spectrometer operating within the mid-infrared (MIR) range of 4000–400 cm^{-1}. The elemental composition of the biochar was assessed by X-ray fluorescence spectroscopy (XRF) with a Rigaku ZSX Primus II instrument, while crystallinity was determined using X-ray diffraction (XRD) via a Rigaku Ultima-IV diffractometer scanning over a 2θ range of 0–90°. The surface morphology and microstructural features were examined using scanning electron microscopy (SEM) with a Quanta 400F field emission system, equipped with energy-dispersive X-ray spectroscopy (EDX). The particle size distribution was analyzed with a Malvern Mastersizer 2000, providing detailed information on the granulometric profile of the biochar. The specific surface area was determined through nitrogen (N_2) adsorption using the Brunauer–Emmett–Teller (BET) method with a Quantachrome Autosorb-6 instrument. Zeta potential analysis was conducted to evaluate the surface charge and colloidal stability of the biochar in aqueous suspension; potential implications for environmental interactions were discussed cautiously and not interpreted as direct evidence of adsorption performance[8].

3. Results and discussion

3.1 FT-IR Analysis of biochar samples

FT-IR spectroscopy was utilized to provide information on the chemical bonds and surface functional groups present in biochar derived from corn stalks, rice husks and the 1:1 (w/w) mixture of these two feedstocks (Figure 1). The spectra also illustrate how biomass structure changes during pyrolysis and the distribution of functional groups within the resulting

carbon matrix. All biochar samples contain one broad absorption band in the 3300–3400 cm^{-1} region caused by O-H stretching vibrations that typically originate from hydroxyl groups on phenolic compounds and residual water. The lower intensity and narrowing of this band for the 1:1 mixture biochar would indicate a decrease in free hydroxyl functional groups due to dehydration/condensation reactions occurring during the co-pyrolysis of the biomass mixtures. The bands at about 2920 and 1420 cm^{-1} are indicative of aliphatic C-H stretching and bending vibrations respectively. In reference to these bands, the reduced intensity of their presence in the mixed biochar products relative to their original sources indicates ongoing degradation of aliphatic compounds and creation of more-ordered (i.e., condensed) carbon structures following thermal conversion. The thermal degradation/reorganisation that occurs in the volatile fractions produced from both feedstocks during co-pyrolysis can lead to a reorganisation of their structural components within their respective carbon matrices. The absorption band at approximately 1580–1610 cm^{-1} can result from either C=O stretching and/or aromatic C=C stretching vibrations, thus representing the presence of both carbonyl and aromatic functional groups within the respective biochar products. The continuance of this band across all of the biochar/mixture products indicates that there is a relative degree of stability of these functional groups at the conditions under which they were produced by pyrolysis. Distinct peaks that occur around 1070 cm^{-1} and 780 cm^{-1} are attributable to the Si-O-Si stretching vibration, which signifies that most of the biochars contain SiO_2 mineral constituents (especially, for example, in biochar produced from rice husks). These peaks indicate that the presence of silica-rich biomass materials is derived from the biochar component of the mixture, and that the minerals are retained after co-pyrolysis. The spectral bands below 500 cm^{-1} are indicative of metal–oxygen bonds (e.g., K–O and Ca–O), showing that inorganic materials are bone in the biochar matrix. Overall, the spectral data suggest that during co-pyrolysis the functional groups undergo transformation and redistribution and create a carbon-rich structure with decreased hydroxyl groups, increased carbonyl species, and

retained mineral oxide signal. These changes suggest interaction effects between the two feedstocks during co-pyrolysis rather than a strictly additive behavior. The combined presence of organic functional groups and mineral phases may contribute to the chemical functionality of the resulting biochar. The observed differences are interpreted as interaction effects based on comparative analysis of individual and mixed biochars, rather than a quantitatively defined synergistic enhancement. The observed decrease in oxygen-containing functional groups (e.g., hydroxyl and carboxyl groups) can be attributed to dehydration, decarboxylation, and condensation reactions occurring during pyrolysis, which promote the formation of more aromatic and thermally stable carbon structures[1,17]. The reduction of oxygen-containing functional groups and the increase in aromatic C=C structures indicate progressive carbonization and condensation reactions, leading to the formation of more stable aromatic domains within the biochar matrix[1,4,17]. During co-pyrolysis, volatile compounds released from different feedstocks may interact and contribute to cross-linking reactions within the carbon matrix, although such mechanisms cannot be directly resolved by FT-IR analysis alone[4]. These observations are based on qualitative FT-IR spectral interpretation, and no quantitative spectral deconvolution was performed; therefore, the results should be considered as indicative of interaction effects rather than direct evidence of specific chemical interactions. Similar FT-IR trends (decreased intensity of hydroxyl/carboxyl-related bands with increasing thermal severity or co-processing) have been reported in co-pyrolysis studies, where dehydration and condensation reactions lead to more condensed carbon structures and reduced oxygen-containing functional groups[18]. Similar transformations of oxygen-containing functional groups and increasing aromaticity with thermal treatment have also been widely reported for biochars produced at moderate temperatures, reflecting progressive dehydration, decarboxylation, and structural condensation reactions during pyrolysis[17,19]. Similar structural evolution trends, including loss of oxygen-containing functional groups and increased aromatic condensation, have been widely reported in biochar systems as a

function of thermal treatment severity[1]. These spectroscopic observations indicate structural transformation during pyrolysis and co-pyrolysis processes, reflecting the progressive loss of oxygen-containing functional groups and the formation of more condensed carbon structures. However, FT-IR analysis provides qualitative information, and therefore the interpretation of interaction effects is based on comparative evaluation rather than quantitative confirmation. The observed differences in the mixture biochar are interpreted as interaction effects between the feedstocks based on comparative analysis with individual biochars. The observed differences between individual and mixed biochars were interpreted as interaction effects based on comparative evaluation rather than as a quantitatively defined synergistic effect. Intermediate or moderated values observed in the mixture may also arise from proportional blending of the feedstocks; therefore, these observations should be considered not as definitive evidence of synergy but rather as indicators of combined or interaction-driven behavior. In this context, the results are discussed in terms of combined or interaction-driven behavior rather than quantitatively confirmed synergy. Recent co-pyrolysis studies often report clearer FT-IR-derived interaction claims when supported by peak deconvolution or complementary surface chemistry (e.g., XPS), whereas in the present study the FT-IR-based interpretation is intentionally limited to comparative band-intensity trends at 400 °C, emphasizing temperature-driven carbonization rather than quantified feedstock–feedstock chemical synergy[20,21].

3.2 XRF Analysis of biochar samples

Element and compound on oxide form content of the biochar samples obtained from pyrolysis of rice husk, corn stalk, and their 1:1 (w/w) mixture at 400 °C determined by XRF analysis are given Table 1. XRF analysis identified Si, K, and Ca as the major inorganic compounds in the biochar samples. Among these, Si was particularly abundant in the rice husk-derived biochar (SiO_2 content: 63.7 wt%), while it was significantly lower in the corn stalk-derived biochar (21.0 wt%). The current study's result is

consistent with the results of other studies that indicate that rice husks are naturally very high in SiO_2, with most of this SiO_2 remaining in the biochar matrix following pyrolysis[22]. The mixture biochar contained an intermediate amount of SiO_2 (47.8 wt%), which indicates a combination of contributions from rice husk (from the high SiO_2 rice husk) and corn stalks (the low SiO_2 feedstock). Besides Si, the mixture biochar also contained a significant amount of K_2O (17.3 wt%) and CaO (13.9 wt%), indicating that K and Ca derived from the corn stalk were retained in the biochar matrix. The relative mineral composition of the biochar (and, therefore, the interaction effects associated with co-pyrolysis) suggests that during co-pyrolysis of the two feedstocks, the inorganic characteristics of both feedstocks combined with one another in the final biochar matrix; thus, the mineral composition trends observed were considered as interaction effects arising from the combined contribution of both feedstocks rather than quantitatively verified synergistic enhancement. Lignocellulosic feedstock co-pyrolysis studies have shown that utilizing lignocellulosic mixtures will add their respective mineral characteristics to one single composite; this will impact upon the resulting ash's mineralogical composition and ash mineral retention on the basis of temperature and mixture composition[7]. During co-pyrolysis, the integration of mineral phases may occur due to a redistribution of the inorganic components that are los during thermal decomposition (volatiles are lost due to volatilisation, melting, and reprecipitated to allow the incorporation of minerals into the carbon based on the carbon structure), which has the potential to affect the mineral chemistry and retain inside biochar due to the stability of the resulting structure[4,23]. In addition to that, alkali and alkaline earth metals can serve as a catalyst in pyrolysis thereby affecting devolatilization and providing structural rearrangement of the resulting carbon matrix along with affecting the final mineral distributions and stability[6]. Research shows that the composition of minerals in biochar is directly affected by the type of feedstock used - rice husk or other silica content being significant contributors to ash content versus higher alkali and alkaline earth content found in herbaceous materials[4,23]. Likewise,

recent studies have further emphasized the impact of feedstock on the chemistry of ash and the chemistry of ash forged during pyrolysis, which demonstrates that there are many different chemical forms contained in all feedstock and their accumulation in biochar results from how the feedstock was processed[6]. The balanced nature of these mineral compositions may enhance the agronomic value of biochar by providing nutrient availability, cation exchange capacity and improving the structure of the soils in which biochar is used. Potassium and calcium aid in soil fertility through nutrient cycling and improvements to soil structure. Additionally, although Si may not be essential for the growth of many crops, it does provide advantages relating to the plants' resistance to abiotic and biotic stresses, including droughts, salinity and diseases caused by pathogens. The minor but functionally relevant levels of other oxides, such as Fe_2O_3 (6.47 wt, %), Al_2O_3 (3.29 wt, %), and MgO (1.88 wt, %), further indicate the stable incorporation of trace minerals into the biochar matrix. Furthermore, the alkaline nature of the biochar ($pH = 7.69 \pm 0.06$), supported by these mineral constituents, can be beneficial for pH regulation and microbial activity enhancement in acidic soils[24,25]. These observations are also supported by FT-IR and XRD analyses, which confirm the retention of mineral oxide phases in the biochar matrix. In summary, the XRF results corroborate the multifunctional agronomic potential of the co-pyrolyzed biochar and highlight the integrated mineral profile achieved by blending biomass types with complementary inorganic compositions[7]. The observed differences are interpreted as interaction effects based on comparative analysis of individual and mixed biochars, rather than a quantitatively defined synergistic enhancement. The observed differences in the mixture biochar are interpreted as interaction effects between the feedstocks based on comparative analysis with individual biochars. In this context, the results are discussed in terms of combined or interaction-driven behavior rather than quantitatively confirmed synergy. Recent studies have shown that co-pyrolysis can significantly alter mineral retention and ash composition, particularly at higher temperatures where mineral transformation and volatilization are more pronounced[6,7]. In contrast, the

present study indicates that at moderate pyrolysis temperature (400 °C), the mineral composition of the mixture biochar largely reflects the proportional contribution of individual feedstocks, suggesting limited mineral transformation and redistribution. This observation highlights that temperature plays a dominant role in controlling mineral interactions during co-pyrolysis.

3.3. Particle size distribution of biochar samples

Particle size distribution is a critical parameter influencing the surface area, porosity, and mechanical behavior of biochar. In this study, particle size analyses were performed on biochars derived from corn stalk, rice husk, their 1:1 (w/w) mixture and the results are presented in Figure 2. Particle size distribution parameters are presented as mean values with standard deviations (n = 3), allowing for a more reliable comparison among samples. The inclusion of replicate measurements and standard deviation values provides a quantitative assessment of variability and demonstrates that the observed differences among samples are consistent within experimental uncertainty. The close overlap of replicate distributions further confirms the reproducibility of the particle size measurements. The comparative analysis of particle size distribution parameters for biochar samples given in Table 2 provides essential insights into the influence of biomass type and combined influence leading to higher coarse fraction on particle structure and distribution. The particle size characteristics of biochars produced from rice husk, corn stalk, and their 1:1 mixture reveal notable interaction effects arising from co-pyrolysis. In the mixture biochar, the volume-weighted mean diameter increased to 80.75 ± 3.52 µm, surpassing both rice husk-derived biochar (63.16 ± 2.84 µm) and corn stalk-derived biochar (46.47 ± 2.15 µm), indicating a combined influence leading to higher coarse fraction in coarse particle formation. Similarly, the surface-weighted mean diameter in the mixture reached 21.13 ± 1.04 µm, higher than either individual feedstock, suggesting a shift toward structurally bulkier particles with potentially increased microstructural complexity. Although the d(0.1) value of the mixture (9.67 ± 0.34 µm)

remained relatively close to those of the single-feedstock biochars (9.35 ± 0.31 μm for rice husk and 8.75 ± 0.28 μm for corn stalk), both d(0.5) and d(0.9) values exhibited marked increases 49.61 ± 2.15 μm and 176.48 ± 7.21 μm respectively highlighting a broadened distribution toward larger particle sizes. These shifts confirm that the particle size distribution widened significantly upon mixing, with an overall increase in the size range towards larger particles. The sharp rise in d(0.9) particularly highlights the development of a substantial fraction of coarse particles in the mixed biochar sample. This trend is quantitatively supported by the SPAN value of 3.36 ± 0.14 in the mixture, which is significantly higher than in rice husk (2.89 ± 0.12) and corn stalk (2.06 ± 0.09) biochars, reflecting increased particle-size heterogeneity relative to individual feedstocks. These observations confirm that the co-pyrolysis of rice husk and corn stalk induced combined influence of both feedstocks on the particle size distribution, enhancing the structural diversity of the biochar. Such characteristics in the mixture biochar may be relevant for applications where both fine and coarse particle fractions influence surface accessibility and particle interactions. The broader particle size distribution may influence functional behavior by affecting surface accessibility and particle interactions, which are known to play a key role in adsorption and soil–biochar interactions[1,4,26]. These results indicate that the co-pyrolysis of rice husk and corn stalk led to changes in particle size distribution, likely due to interactions between thermally decomposed biomass components. The broadened distribution and increased particle size may be associated with aggregation and structural rearrangement during thermal conversion rather than a purely additive effect. The observed changes in particle size distribution may be associated with thermal softening, fragmentation, and aggregation processes occurring during pyrolysis. The interaction of devolatilized organic components and molten mineral phases can promote particle coalescence, leading to the formation of larger aggregates and a broader size distribution[26,27]. In addition, mineral melting and ash-mediated binding have been reported to enhance particle agglomeration during thermal conversion, particularly in lignocellulosic biomass systems,

contributing to increased heterogeneity in particle size distribution[18,23]. Comparable co-processing studies have shown that blending components can broaden particle-size distributions due to aggregation and melt/ash-mediated binding during thermal conversion, resulting in coarser fractions even when surface area is partially preserved[18]. Particle size distribution in biochars has also been reported to be influenced by both feedstock structure and pyrolysis conditions, where lignocellulosic composition and thermal degradation behavior govern fragmentation, aggregation, and pore collapse mechanisms[26,27]. Recent co-pyrolysis studies further suggest that interactions between biomass components can alter fragmentation behavior and promote particle aggregation, depending on thermal decomposition pathways and mineral content[5]. Compared with recent co-pyrolysis studies reporting particle-size narrowing under higher-temperature treatments due to intensified fragmentation, the present results show a pronounced widening of the distribution (SPAN = 3.36 ± 0.14) at 400 °C, suggesting that aggregation/coalescence processes can dominate over fragmentation under moderate thermal severity and mineral-rich conditions[5,18,23].

3.4. Specific surface area results of biochar samples

The BET surface area of the biochar mixture produced from rice husk and corn stalk was 13.17 ± 0.42 m^2 g^{-1}, indicating a considerable level of surface development despite the observed increase in particle size and distribution heterogeneity. Individually, the rice husk-derived biochar and corn stalk-derived biochar exhibited specific surface areas of 13.90 ± 0.35 m^2 g^{-1} and 11.96 ± 0.28 m^2 g^{-1}, respectively. The values are expressed as mean ± standard deviation (n = 3). Although the differences among samples are relatively small, the inclusion of standard deviation provides a more reliable basis for comparison and indicates that the observed variations fall within the range of experimental variability. The rice husk biochar, with its finer particle size distribution and relatively broader SPAN, contributed a greater initial surface area, while the corn stalk biochar, though slightly lower in SSA, likely enhanced structural uniformity

through its more homogeneous fragmentation profile. The mixture biochar, although it displayed the coarsest particle characteristics reflected by the highest volume-weighted mean diameter (80.749 µm) and SPAN (3.362) retained a surface area comparable to that of the rice husk biochar. This result suggests that the finer fraction and porous architecture of the rice husk may have played a dominant role in determining the final surface properties of the mixture, whereas the corn stalk component potentially contributed to microstructural rearrangements that helped stabilize surface area despite particle coarsening. Therefore, the resulting surface area of 13.17 ± 0.42 m^2 g^{-1} can be interpreted as a balanced outcome of the combined influence of both feedstocks, in which the structural advantages of both biomass types are successfully integrated. This combination yields a material with enhanced pore accessibility and broadened particle size distribution, offering physicochemical characteristics that may support surface-dependent applications (e.g., adsorption-related processes); however, adsorption or remediation performance cannot be concluded from BET surface area alone and should be verified experimentally. Similar combined influence of both feedstocks between biomass components leading to preserved or enhanced surface area despite particle coarsening have also been reported in the literature[13,14]. However, the relatively moderate surface area can be attributed to the low pyrolysis temperature (400 °C), which is known to limit pore development compared to higher temperatures. The development of surface area and porosity in biochar is primarily governed by devolatilization and structural rearrangement processes during pyrolysis. The release of volatile compounds creates pore networks within the carbon matrix, while simultaneous structural shrinkage and collapse may limit pore development at moderate temperatures[1,17]. The evolution of pore structure is also associated with the development of micro- and mesopores during thermal decomposition, where the release of volatiles generates initial microporosity, while subsequent structural rearrangement and pore widening contribute to mesopore formation. These processes are strongly influenced by temperature and feedstock

composition, particularly in co-pyrolysis systems[1,2,28]. In co-pyrolysis systems, interactions between different biomass components may further influence pore evolution by modifying thermal decomposition pathways and mineral distribution, which can affect pore accessibility and structural stability of the resulting biochar[4,18]. It should be noted that surface area alone does not directly determine adsorption performance, as sorption processes are influenced by multiple factors including pore size distribution, surface functional groups, and solution chemistry[1,2]. Therefore, the contribution of surface area to adsorption behavior should be interpreted cautiously, rather than as a direct indicator of functional performance. The observed differences in the mixture biochar are interpreted as interaction effects between the feedstocks based on comparative analysis with individual biochars. It should be noted that intermediate or moderated values may also arise from proportional blending of the components, and therefore these observations should not be considered as definitive evidence of synergistic enhancement. In this context, the results are discussed in terms of combined or interaction-driven behavior rather than quantitatively confirmed synergy. In this study, a predictive baseline (e.g., weighted-average/additive model) was not applied to quantify deviations from blending behavior; therefore, the observed intermediate properties are discussed as interaction/combined effects based on comparative evaluation rather than statistically confirmed synergy. Recent work also indicates that BET surface area commonly increases with higher pyrolysis temperatures, whereas moderate temperatures (e.g., ~400 °C) often yield comparatively lower SSA due to limited pore development, supporting a cautious interpretation of adsorption implications[28]. Numerous studies have demonstrated that biochar surface area increases with pyrolysis temperature due to enhanced devolatilization and pore formation, while lower temperatures typically result in limited porosity development and lower surface areas[1,2]. It has also been reported that the development of porosity in biochar is strongly influenced by devolatilization processes and structural collapse, which are controlled by both feedstock type and pyrolysis temperature[4]. Recent co-

pyrolysis studies have reported that blending lignocellulosic feedstocks can lead to either enhanced or reduced surface area depending on synergistic interactions, ash content, and thermal conversion pathways[7,13,14]. In the present study, the mixture biochar exhibited a surface area (13.17 ± 0.42 m^2 g^{-1}) comparable to that of rice husk biochar despite increased particle size, suggesting that pore development was partially preserved under the applied conditions. This behavior differs from studies reporting significant surface area enhancement at higher temperatures, indicating that at moderate pyrolysis temperatures (400 °C), structural rearrangement and pore collapse may limit surface development. These findings highlight that the interaction effects observed in this study are primarily governed by temperature-controlled thermochemical processes rather than strong synergistic enhancement, contributing to a more nuanced understanding of co-pyrolysis behavior.

3.5. Zeta potential results of biochar samples

Zeta potential is a fundamental physicochemical parameter reflecting the surface charge and colloidal stability of biochar particles in aqueous medium. Zeta potential measurements were conducted for biochars obtained from corn stalk, rice husk, and their 1:1 (w/w) mixture, with the results summarized in Figure 3. The zeta potential measurements revealed notable differences in surface charge among the biochar samples. The biochar derived from corn stalk exhibited the most negative zeta potential (−33.7 ± 1.2 mV), indicating high colloidal stability and stronger electrostatic repulsion among particles. Rice husk-derived biochar showed a slightly less negative value (−27.2 ± 1.0 mV), suggesting moderate stability in suspension. Interestingly, the zeta potential of the 1:1 (w/w) mixture was measured as (−25.7 ± 1.3 mV), less negative than either of the individual biochars. The values are expressed as mean ± standard deviation (n = 3). Although the differences among samples are relatively small, the inclusion of standard deviation allows for a more reliable comparison and indicates that the observed variations fall within the range of experimental variability. This shift indicates a potential reduction in

colloidal stability and suggests surface charge neutralization or interaction effects during co-pyrolysis. The observed change in surface charge may be attributed to the redistribution of functional groups or alterations in mineral content at the particle interface. Such changes in surface charge may influence interactions with charged species in aqueous systems and soil environments; however, adsorption performance cannot be inferred from zeta potential alone. The negative zeta potential values indicate that the biochars possess net negative surface charges under neutral conditions, likely due to the presence of deprotonated oxygen-containing functional groups such as carboxyl and phenolic groups formed during pyrolysis[29,30]. Surface charge development in biochar is strongly related to the dissociation of oxygen-containing functional groups and the distribution of mineral phases, both of which are influenced by pyrolysis conditions and feedstock composition[1,4,30,31]. Recent co-pyrolysis studies report that ζ-potential can become more negative when oxygenated functional groups are preserved or generated, whereas the slightly less negative ζ of the mixture in this study (−25.7 ± 1.3 mV) relative to the single-feedstock biochars suggests that mineral-phase contributions and partial charge screening may outweigh functional-group-driven negative charge development under the applied conditions (400 °C, 1:1 blend). However, the relationship between zeta potential and adsorption performance should be interpreted cautiously, as surface charge alone does not directly determine adsorption capacity. It should be noted that zeta potential primarily reflects surface charge characteristics and colloidal stability, and does not directly quantify adsorption capacity. Although surface charge may influence interactions with charged species in aqueous systems, adsorption behavior of biochar is governed by a combination of factors including surface functional groups, mineral composition, and pore structure[29,30]. Therefore, interpretations relating zeta potential directly to adsorption performance should be considered cautiously. Recent research on biochar colloids highlights that zeta potential is a dominant control on colloidal mobility under varying ionic strength, reinforcing that ζ-potential primarily reflects electrostatic

behavior and stability rather than directly quantifying adsorption capacity[8]. It is also well established that biochar surface charge is largely controlled by oxygen-containing functional groups and mineral components, which influence electrostatic interactions in aqueous systems[30,31]. Recent studies have further emphasized that electrostatic interactions and surface functional groups jointly control the behavior of biochar particles in aqueous systems, particularly under varying pH and ionic strength conditions[2]. Recent studies have shown that more negative zeta potential values are often associated with higher densities of oxygen-containing functional groups, whereas the less negative value observed in the mixture biochar suggests that mineral-induced charge screening and surface heterogeneity may counterbalance functional-group-driven surface charge development[8,30,31].

3.6. SEM Analysis results of biochar samples

The physical morphology of the biochar samples was examined using SEM, and the corresponding micrographs and energy-dispersive X-ray (EDX) spectra are presented in Figure 4. SEM observations were performed on multiple randomly selected regions of each biochar sample to ensure that the presented micrographs are representative of the overall surface morphology. SEM images and EDX spectra reveal distinct morphological and elemental characteristics for the biochars obtained from corn stalk, rice husk, and their 1:1 (w/w) mixture. Semi-quantitative elemental compositions were obtained from EDX analysis at multiple measurement points (n = 3), and the values are reported as mean percentages. Biochar from corn stalks has rough surfaces, cavities scattered everywhere on it, and burned particles suggesting it is moderately porous. EDX demonstrated a majority of C atoms, with smaller amounts of O, Si, and traces of K indicating that the biochar retained only some of the minerals originally in the biomass. In contrast the rice husk biochar shows a much more orderly sheet-like microstructural form, with some surface areas being much smoother; EDX demonstrates very similar elemental compositions, although the Si intensity was much greater and is consistent

with the rice husk's highly siliceous nature. Lastly, the mixed biochar displays a much more heterogeneous-type of surface morphology, consisting of both fragmented and porous surface features. SEM photographs of the co-pyrolyzed mixture demonstrate that the highly varied textural complexity associated with the carbonaceous matrix, which has well defined, visible pore networks, along with brighter regions that correspond to inclusions of gaseous oxygen and minerals, such as metal oxides. Results of EDX analysis revealed the predominant chemical composition of the mixed sample consisted primarily of carbon and oxygen, followed by significant amounts of Si and K, corroborating that the two biomass sources contributed to a composite mineral composition within the mixture. Subsequently, the structural and/or compositional features, which were found in the mixture sample, support that there were significant structural changes that occurred due to the interaction of the feedstocks during the pyrolysis process. The combination of the rice husk, which has a high silica content, together with the corn stalk, which contains a high carbon content, appears to result in the creation of a biochar product that contains even more irregular surfaces than either of the feedstocks alone, suggesting that this product may provide greater surface area access and surface interactions with environmental systems than either feedstock alone would provide. The observed heterogeneous morphology may result from differential thermal decomposition of biomass components, where the release of volatiles and the redistribution of mineral phases contribute to pore formation, structural collapse, and reorganization of the carbon matrix[1,4,17,23]. Unlike co-pyrolysis studies at higher temperatures that report more uniformly developed pore networks linked to stronger devolatilization-driven porosity, the present SEM observations at 400 °C indicate a mixed-domain morphology (fragmented + mineral-inclusion regions), consistent with partial carbonization and ash-mediated restructuring rather than uniformly enhanced pore development. As previously noted, the porous structure observed in the SEM images, along with the moderate surface area revealed by BET analysis, indicates that the mixture biochar produced at 400 °C possesses favorable

physicochemical properties for environmental applications. These physicochemical features suggest that the material may be suitable for use as a soil amendment (e.g., as a pH-buffering and mineral-containing amendment); however, its agronomic performance (nutrient retention, plant response, and soil microbial effects) should be confirmed by soil-based experiments. These structural characteristics suggest that the biochar may have potential for applications such as soil amendment and environmental remediation; however, further application-based studies are required to confirm its performance. However, these interpretations are based on physicochemical characterization and should be considered as indicative rather than definitive without application-based validation[1,2,4,32]. Co-pyrolysis literature similarly reports that blending can increase morphological heterogeneity and mineral dispersion, which may affect surface accessibility; however, these observations should be treated as structural indicators unless validated by application-specific tests[7]. Similar heterogeneous morphologies and pore structures have been widely observed in biochars derived from lignocellulosic biomass, where thermal decomposition leads to the formation of irregular pore networks and mineral inclusions[4,26]. Morphological heterogeneity and pore development have been reported to play a critical role in determining biochar reactivity, particularly in relation to adsorption and soil interactions[1]. Unlike studies conducted at higher temperatures where more uniform pore networks are formed due to intensified devolatilization, the heterogeneous morphology observed in this study reflects partial carbonization and mineral–organic interactions typical of moderate-temperature pyrolysis[1,7,17].

3.7. XRD Analysis results of biochar samples

The microcrystalline structure of the biochar samples was examined using XRD over a 2θ range of 0–90° (Figure 5). The diffraction patterns of biochars derived from corn stalk (Figure 5a), rice husk (Figure 5b), and their 1:1 (w/w) mixture (Figure 5c) exhibit diffraction features characteristic of predominantly amorphous carbon matrices with embedded and retained mineral phases. In the corn stalk-derived biochar

(Figure 5a), the diffraction profile is dominated by a broad hump centered at 2θ ≈ 20–30°, which is commonly attributed to disordered aromatic carbon domains formed during the thermal degradation of cellulose, hemicellulose, and lignin[17,23]. The absence of sharp and therefore crystalline like cellulose-related diffraction peaks as well as the lack of an intense graphitic diffraction peak, indicate that a high degree of loss of structural order and incommensurate graphitization has occurred. The results provide confirmation that the carbon phase consists primarily of turbostratic (or amorphous) structures typical for biochars produced via pyrolysis at low temperatures (~400 °C)[1,2]. Only minor diffraction reflections corresponding to crystalline materials were found, indicating that there is only a minimal amount of inorganic minerals present. Similar to other studies, the majority of carbon in the biochars produced at these temperatures consists of amorphous carbon with a residual quantity of mineral materials[17,23]. Rice husk-derived biochar (Figure 5b) exhibited a relatively large quantity of amorphous carbon with an associated broad halo, but also featured a single sharp reflection at ~28 degrees 2θ that was associated with crystalline silica (SiO_2) - supporting the high concentration of silica in rice husk-derived biomass. The continued presence of crystalline silica (especially) indicates that the mineral phase remains thermally stable after processing. Additional smaller peaks due to K and Ca (alkali and alkaline earth metals) in mixed feedstocks also demonstrate the presence and distribution of inorganic compounds while converting to biochar (thermochemical)[6,23]. Biochars created using different types of feedstocks have unique structural characteristics that can be recognized by their basal amorphous C peaks (Figure 5) and Si crystalline diffraction peaks from the original rice husk mineral and crystalline materials retained throughout the co-pyrolysis process; however, for co-pyrolyzed (mixed) biochar, some of the characteristic reference diffractions from the co-feedstock's biochars are less pronounced (have lower relative intensity than their co-feedstock's biochars individual samples) and broader than their reference diffractions (indicating greater structural disorder) and suggests that redistribution of minerals potentially has occurred[4,6,7].

Previous research has identified comparable trends between the structural evolution associated with cooperative pyrolysis and the interactions between the organic matrix and mineral constituents associated with the organic feedstock; furthermore, these interactions affect the location and type of carbon ordered, promote mineral-catalyzed reactions and redistribute minerals from phase aligned among multiple biochar products. Thus, associated with the above-mentioned mineral-organic interactions, the final carbon matrix will exhibit a more homogeneously structured and disordered carbon matrix. Thermal degradation of cellulose, hemicellulose, and lignin results in the formation of amorphous carbon structures during pyrolysis due to the destruction of crystalline order and the formation of disordered, aromatic systems[17,23]. A biochar produced via pyrolysis at a moderate temperature generally has little to no crystalline carbon and contains predominantly amorphous carbon5, while surface reactivity is generally enhanced due to its predominance of amorphous characteristics[1,2,32]. However, functional properties associated with the biochar (e.g., adsorption, contaminant binding, soil amendment) must be validated under specific testing conditions[7]. Results of XRD analysis indicate that co-pyrolysis at 400 °C results in a greater degree of structural homogeneity and an increase in amorphous character in comparison to the use of individual feedstocks. In contrast to most co-pyrolysis studies that have quantified crystallinity changes using peak deconvolution or crystallinity index calculation and statistically supported temperature-dependent increases in amorphousness, the current study's interpretation uses only qualitative evaluation of peak broadening and relative intensity differences as a measure of amorphousness. It's worth noting that no crystallinity index calculations, peak area integrations, peak deconvolutions, or Rietveldg refinements were conducted in this study[20,33,34]. Quantitative methods for assessing crystallinity of carbonaceous materials typically require sophisticated analytic methods (e.g., Rietveldg refinement, crystallinity index calculation), so the observed differences in the samples can be viewed as signs of structural differences,

but do not provide quantitatively-confirmed evidence of increases in amorphization.

3.8. Characterization of the mixture biochar

Table 3 presents data on selected physicochemical characteristics of the biochar, as derived from corn stalk, rice husk, and their 1:1 (w/w) mixture. These characteristics provide essential information about the chemical makeup, nutrient makeup, and potential agronomic function(s) of the resulting biochar products. The moisture content of each of the biochars was between 3.28 to 3.50% and could be classified as relatively dry and stable. This moisture content is typical of biochars produced by controlled pyrolysis methods and is a positive characteristic for both the long-term use of the biochar in storage and for efficient application to soil. Similar moisture contents have been reported for agricultural residue-derived biochars produced at medium temperature ranges[1,4]. The organic matter contents of the biochars were all fairly high, ranging from 64.87% to 75.49%, and indicate that the original source materials were primarily made up of carbon-based materials. The corn stalk biochar had the highest organic matter content, while the facility's biochar had somewhat lower (64.87%) organic matter content due to the presence of a higher amount of mineral content from the rice husk ash. Rice husk biomass is known to have high levels of silica, which can reduce the relative amount of organic carbon in the resulting biochar[4,35]. The pH of the biochar was measured at 7.52 ± 0.05 – 7.84 ± 0.04, and the pH of the mixture biochar was 7.69 ± 0.06. Since the pH is slightly alkaline, this is what you would typically expect for biochars made at moderate pyrolysis temperatures. The observed trend agrees with the behavior of biochar made at moderate temperatures. The thermal decomposition of acidic functional groups and the deposition of alkali-forming minerals such as carbonates, oxides and silicates shifts the pH upwards; therefore, higher pH levels will likely help acid soils in terms of their ability to buffer and create better living conditions for microorganisms[36,27]. The electrical conductivity for the biochars is between 4.70 and 5.80 dS m^{-1}; therefore, the biochar contains

a moderate amount of soluble salts. The mixture biochar displayed an intermediate EC value (5.62 dS m^{-1}), reflecting the combined mineral contributions of both feedstocks. According to literature, EC levels between 2 and 10 dS m^{-1} are generally considered safe for agricultural use and pose minimal salinity risk to most crops, including salt-sensitive species[15]. The EC level indicates that the produced biochar poses no significant salinity risk to soil or plants, including salt-sensitive crops. Moreover, the presence of soluble minerals may contribute to nutrient enrichment when applied to soil. The nutrient-related parameters further demonstrate the agronomic potential of the produced biochars. The total nitrogen content ranged from 0.84% in corn stalk biochar to 1.32% in the mixture biochar, suggesting that co-pyrolysis may enhance nitrogen retention compared with single feedstock biochar. Nitrogen retention during pyrolysis is influenced by biomass composition and interactions between organic components during thermal decomposition[1]. Similarly, the biochars contained appreciable amounts of total P_2O_5 and total K_2O. The P_2O_5 content ranged between 1.16 and 1.23%, while K_2O varied from 1.50 to 1.76%. The fertilizing property of biochar is increased when added to soil due to the nutrient content necessary for plant growth[4]. The K content of biochar from corn stalks was 1.76%, which is consistent with past research showing that herbaceous crops produce residual K during production[30]. Sulphur was present as SO_3 (0.28–0.33%) in biochar and indicates that pyrolized biological material retained sulphur containing minerals. The sulphur found in biochar can assist in providing sulphur to the soil, an important nutrient for plant processes and protein formation. Overall, the biochar produced from mixing rice husks and corn stalks had a balanced physicochemical makeup, having a moderate level of alkalinity, containing mineral nutrients, and moderate to high quantity of natural organic material. These characteristics lead to the conclusion that biochar created by co-pyrolysis of rice husk and corn stalk should have desirable characteristics for soil amendment. Again, as indicated by the previous studies, the agronomic performance of biochar is influenced by its own physicochemical properties, but also by the type of soil, the environment,

and the application rate[4,32]. Earlier studies have documented the ability of biochar to improve physical, chemical, and biochemical soil qualities across a variety of climatic conditions, as well as enhance the growth and yield of crops. In an earlier study by Demir[11], it was reported that applying a 1:1 (w/w) blend of biochar increased the physiological response of silage maize grown on drip irrigation. Similarly, in the study by Demir and Bayraklı[12], it was reported that applying a 1:1 (w/w) blend of biochar improved the physical and chemical properties of the soil, as well as the yield of silage maize and the efficiency with which water was used, under drought conditions. These results serve as a performance-based example of the agronomic importance of using biochar to amend soils.

4. Conclusion

This study provides a comprehensive physicochemical characterization of biochar produced through the co-pyrolysis of rice husk and corn stalk, with a particular focus on the combined influence of both feedstocks arising from biomass mixture. The combined application of FT-IR, XRD, SEM–EDX, XRF, BET, particle size, and zeta potential analyses revealed that the mixture biochar exhibits a structurally complex, chemically enriched, and exhibits a structurally complex and chemically enriched profile based on physicochemical characterization compared to the biomass alone. Notably, the integration of silica-rich rice husk and nutrient-dense corn stalk resulted in a biochar with resulted in a biochar with an integrated mineral composition, expanded particle size distribution, retained surface area, and moderated surface charge, indicating a combined influence of both feedstocks during thermal decomposition. The obtained biochar suggests integrated structural and chemical characteristics, which may provide potential for environmental and agricultural applications. However, these interpretations are based on physicochemical characterization results and should be considered as indicative rather than definitive. In particular, its physicochemical properties suggest possible benefits in soil amendment, such as nutrient retention and pH buffering; however, these implications require further experimetal validation under practical conditions. Beyond

the properties of individual biomass types, this study highlights that co-pyrolysis can influence biochar characteristics through interactions between feedstocks. These findings contribute to a better understanding of biomass utilization strategies and support the development of biochar materials for sustainable resource management based on physicochemical characterization, while performance under realistic application conditions remains to be validated. These findings suggest that co-pyrolysis influences biochar properties through coupled thermochemical processes, including devolatilization, condensation, pore development, and mineral redistribution.

Funding

This study was financially supported by the TAGEM (General Directorate of Agricultural Research and Policies) of Ministry of Agriculture and Forestry of Republic of Türkiye (with the project number of TAGEM/TSKAD/B/21/A9/P2/2772).

Acknowledgement

The author would like to thank the Republic of Türkiye Ministry of Agriculture and Forestry General Directorate of Agricultural Research and Policies (TAGEM) for the financial support for the Project TAGEM/TSKAD/B/21/A9/P2/2772. The authors would like to thank editors and the anonymous reviewers for the helpful comments, corrections, and suggestions on the previous version of the manuscript

Data availability

Data is provided within the manuscript or supple mentary information files.

Authorship contribution

Zeynep Demir: Project administration, Conceptualization, Methodology, Data curation, Formal analysis, Investigation, Statistic, Resources, Software, Supervision, Validation, Visualization,

Writing – review and editing. **Pınar Acar Bozkurt:** Writing – review and editing.

Conflicts of Interest

The author declare no conflicts of interest.

Ethics approval and consent to participate

Not applicable.

REFERENCE

1. Ahmad, M., Lee, S. S., Dou, X., Mohan, D., Sung, J. K., Yang, J. E. & Ok, Y. S. Effects of pyrolysis temperature on sorption of heavy metals by biochar: A review. *Bioresource Technology*, **155**, 1–12 (2014).
2. Tan, X., Liu, Y., Zeng, G., Wang, X., Hu, X., Gu, Y. & Yang, Z. Application of biochar for the removal of pollutants from aqueous solutions. *Chemosphere*. Apr; **125**, 70-85. https://doi.org/10.1016/j.chemosphere.2014.12.058 (2015).
3. Mohan, D., Sarswat, A., Ok, Y. S. & Pittman Jr, C. U. Organic and inorganic contaminants removal from water with biochar, a renewable, low cost and sustainable adsorbent – A critical review. *Bioresource Technology*, **160**, 191–202. https://doi.org/10.1016/j.biortech.2014.01.120 (2014).
4. Lehmann, J. & Joseph, S. (Eds.). Biochar for Environmental Management: Science, Technology and Implementation (2nd ed.). Routledge. https://doi.org/10.4324/9780203762264 (2015).
5. Chen, H., Cheng, Y., Luo, L., Li, X., Zhang, S. & Zeng, G. Co-pyrolysis of biomass and waste: A review of synergy effects, energy production and environmental impacts. *Journal of Cleaner Production*, **331**, 129967 (2022).
6. Wang, J., Xiong, Z. & Kuzyakov, Y. Biochar stability in soil: Meta-analysis of decomposition and priming effects. *GCB Bioenergy*, **8**(3), 512–523. https://doi.org/10.1111/gcbb.12266 (2019).

7. Gusiatin, M. Z. Advantages of Co-Pyrolysis of Sewage Sludge with Agricultural and Forestry Waste. *Energies*, **17**, 5736. https://doi.org/10.3390/en17225736 (2024).
8. Yin, Y., Yin, R., Sharma, P. & Shang, J. Mobility of biochar colloids from diverse feedstocks: Dominant control of zeta potential under varying ionic strength and Cd^{2+} presence. *Journal of Environmental Management*, **394**, 127361, https://doi.org/10.1016/j.jenvman.2025.127361 (2025).
9. Petrović, J., Koprivica, M., Ercegović, M., Simić, M., Dimitrijević, J., Bugarčić, M. & Trifunović, S. Synthesis and Application of FeMg-Modified Hydrochar for Efficient Removal of Lead Ions from Aqueous Solution. *Processes*. **13**(7), 2060. https://doi.org/10.3390/pr13072060 (2025).
10. Dafalla, M., Inayat, A., Jamil, F. & Ghenai, C. Prospective of biochar material production and process optimization using co-pyrolysis approach- A mini-review. Sharjah International Conference on Physics of Advanced Materials Journal of Physics: Conference Series **2751**, 012024 IOP Publishing https://doi.org/10.1088/1742-6596/2751/1/012024 (2024).
11. Demir, Z. Physiological responses of silage maize to drip ırrigation regimes and biochar applications. *J Plant Growth Regul*. https://doi.org/10.1007/s00344-025-12003-z (2025).
12. Demir, Z. & Bayraklı, B. Effects of biochar on soil chemical, physical, and biochemical properties, silage maize yield, water productivity and economic returns under drought conditions, *Pedosphere.* https://doi.org/10.1016/j.pedsph.2026.02.011 (2026).
13. Zhao, L., Cao, X., Masek, O. & Zimmerman, A. Heterogeneity of biochar properties as a function of feedstock sources and production temperatures. *Journal of Hazardous Materials.* **256–257**, 1–9. https://doi.org/10.1016/j.jhazmat.2013.04.015 (2013).
14. Qian, K., Kumar, A., Zhang, H., Bellmer, D. & Huhnke, R. Recent advances in utilization of biochar. *Renewable and Sustainable Energy*

Reviews. **42**, 1055–1064. https://doi.org/10.1016/j.rser.2014.10.074 (2015).

15. Rajkovich, S., Enders, A., Hanley, K., Hyland, C., Zimmerman, A. R. & Lehmann, J. Corn growth and nitrogen nutrition after additions of biochars with varying properties to a temperate soil. *Biology and Fertility of Soils*. **48**(3), 271-284. https://doi.org/10.1007/s00374-011-0624-7 (2012).
16. American Public Health Association (APHA). Standard methods for the examination of water and wastewater (23rd ed.). APHA, Washington, DC. (2017)
17. Keiluweit, M., Nico, P. S., Johnson, M. G. & Kleber, M. Dynamic molecular structure of plant biomass-derived black carbon (biochar). *Environ Sci Technol*. 2010 Feb 15; **44**(4), 1247-53. https://doi.org/10.1021/es9031419 (2010).
18. Xie, T., Yao, Z., Huo, L., Jia, J., Zhang, P., Tian, L. & Zhao, L. Characteristics of biochar derived from the co-pyrolysis of corn stalk and mulch film waste, *Energy*, Elsevier. **262**, 125554. https://doi.org/10.1016/j.energy.2022.125554 (2023).
19. Sun, K., Kang, M., Zhang, Z., Jin, J., Wang, Z., Pan, Z., Xu, D., Wu, F. & Xing, B. Impact of deashing treatment on biochar structural properties and potential sorption mechanisms of phenanthrene. *Environ Sci Technol*. 2013 Oct 15; **47(20),** 11473-81. https://doi.org/10.1021/es4026744 (2013).
20. Leng, L., Huang, H., Li, H., Li, J. & Zhou, W. Biochar stability assessment methods: A review. *Sci Total Environ*. 2019 Jan 10; **647,** 210-222. https://doi.org/10.1016/j.scitotenv.2018.07.402 (2021).
21. Li, Y., Gupta, R., Zhang, Q., & You, S. Review of biochar production via crop residue pyrolysis: Development and perspectives. *Bioresource Technology*. **369**, 128423, https://doi.org/10.1016/j.biortech.2022.128423 (2023).
22. Xu, G., Lv, Y., Sun, J., Shao, H. & Wei, L. Recent Advances in Biochar Applications in Agricultural Soils: Benefits and Environmental

Implications. *Clean Soil Air Water*. **40,** 1093-1098. https://doi.org/10.1002/clen.201100738 (2012).

23. Enders, A., Hanley, K., Whitman, T., Joseph, S. & Lehmann, J. Characterization of biochars to evaluate recalcitrance and agronomic performance. *Bioresour Technol*. 2012 Jun; **114,** 644-53. https://doi.org/10.1016/j.biortech.2012.03.022 (2012).
24. Yakout, S. M. Physicochemical Characteristics of Biochar Produced from Rice Straw at Different Pyrolysis Temperature for Soil Amendment and Removal of Organics, Proc. Natl. Acad. Sci., India, Sect. A Phys. *Sci*. **87(2),** 207–214. https://doi.org/10.1007/s40010-017-0343-z (2017).
25. Glaser, B., Lehmann, J. & Zech, W. Ameliorating physical and chemical properties of highly weathered soils in the tropics with charcoal – a review. *Biology and Fertility of Soils.* **35(4),** 219–230. https://doi.org/10.1007/s00374-002-0466-4 (2002).
26. Downie, A., Crosky, A. & Munroe, P. Physical Properties of Biochar. In: Lehmann, J. and Joseph, S., Eds., Biochar for Environmental Management: Science and Technology, Earthscan, London, 13-32. (2009)
27. Mukherjee, A., Zimmerman, A. R. & Harris, W. Surface chemistry variations among a series of laboratory produced biochars. *Geoderma.* **163**, 247–255. https://doi.org/10.1016/j.geoderma.2011.04.021 (2011).
28. Suresh Babu, K. K. B., Nataraj, M., Tayappa, M., Vyas, Y., Mishra, R. K. & Acharya, B. Production of biochar from waste biomass using slow pyrolysis: studies of the effect of pyrolysis temperature and holding time on biochar yield and properties. *Mater. Sci. Energy Technol*. **7,** 318–334. https://doi.org/10.1016/j.mset.2024.05.002 (2024).
29. Chen, B., Zhou, D. & Zhu, L. Transitional adsorption and partition of nonpolar and polar aromatic contaminants by biochars of pine needles with different pyrolytic temperatures. *Environmental Science & Technology.* **42**(14), 5137–5143. https://doi.org/10.1021/es8002684 (2008).

30. Yuan, J. H., Xu, R. K. & Zhang, H. The forms of alkalis in the biochar produced from crop residues at different temperatures. *Bioresource Technology*. **102**(3), 3488–3497. https://doi.org/10.1016/j.biortech.2010.11.018 (2011).
31. Uchimiya, M., Lima, I. M., Thomas Klasson, K., Chang, S., Wartelle, L. H. & Rodgers, J. E. Immobilization of heavy metal ions (CuII, CdII, NiII, and PbII) by broiler litter-derived biochars in water and soil. *J Agric Food Chem*. 2010 May 12; **58**(9), 5538-44. https://doi.org/10.1021/jf9044217 (2010).
32. Jeffery, S., Abalos, D., Prodana, M., Bastos, A. C., van Groenigen, J. W., Hungate, B. A. & Verheijen, F. Biochar boosts tropical but not temperate crop yields. *Environ Res Lett.* **12,** 053001. https://doi.org/10.1088/1748- 9326/aa67bd (2017)
33. Bish, D. L. & Post, J. E. *Modern powder diffraction* (2nd ed.). Mineralogical Society of America. (2020).
34. Cheary, R. W., Coelho, A. A. & Cline, J. P. Fundamental Parameters Line Profile Fitting in Laboratory Diffractometers. *J Res Natl Inst Stand Technol*. 2004 Feb 1; **109(1),** 1-25. https://doi.org/10.6028/jres.109.002 (2004).
35. Guo, J. & Chen, B. Insights on the molecular mechanism for the recalcitrance of biochars: interactive effects of carbon and silicon components. *Environ Sci Technol*. 2014 Aug 19; **48(16),** 9103-12. https://doi.org/10.1021/es405647e (2014).
36. Wang, T., Camps-Arbestain, M., Hedley, M., Singh, B. P., Calvelo Pereira, R. & Wang, C. Determination of carbonate-C in biochars. *Soil Research*. **52**, 495-504. https://doi.org/10.1071/SR13177 (2014).

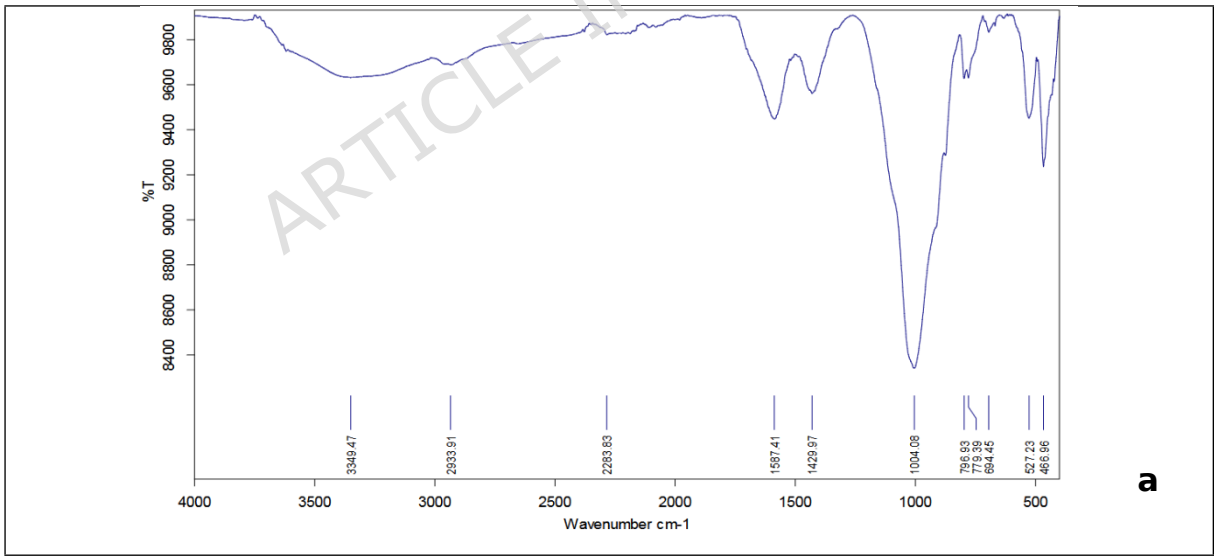

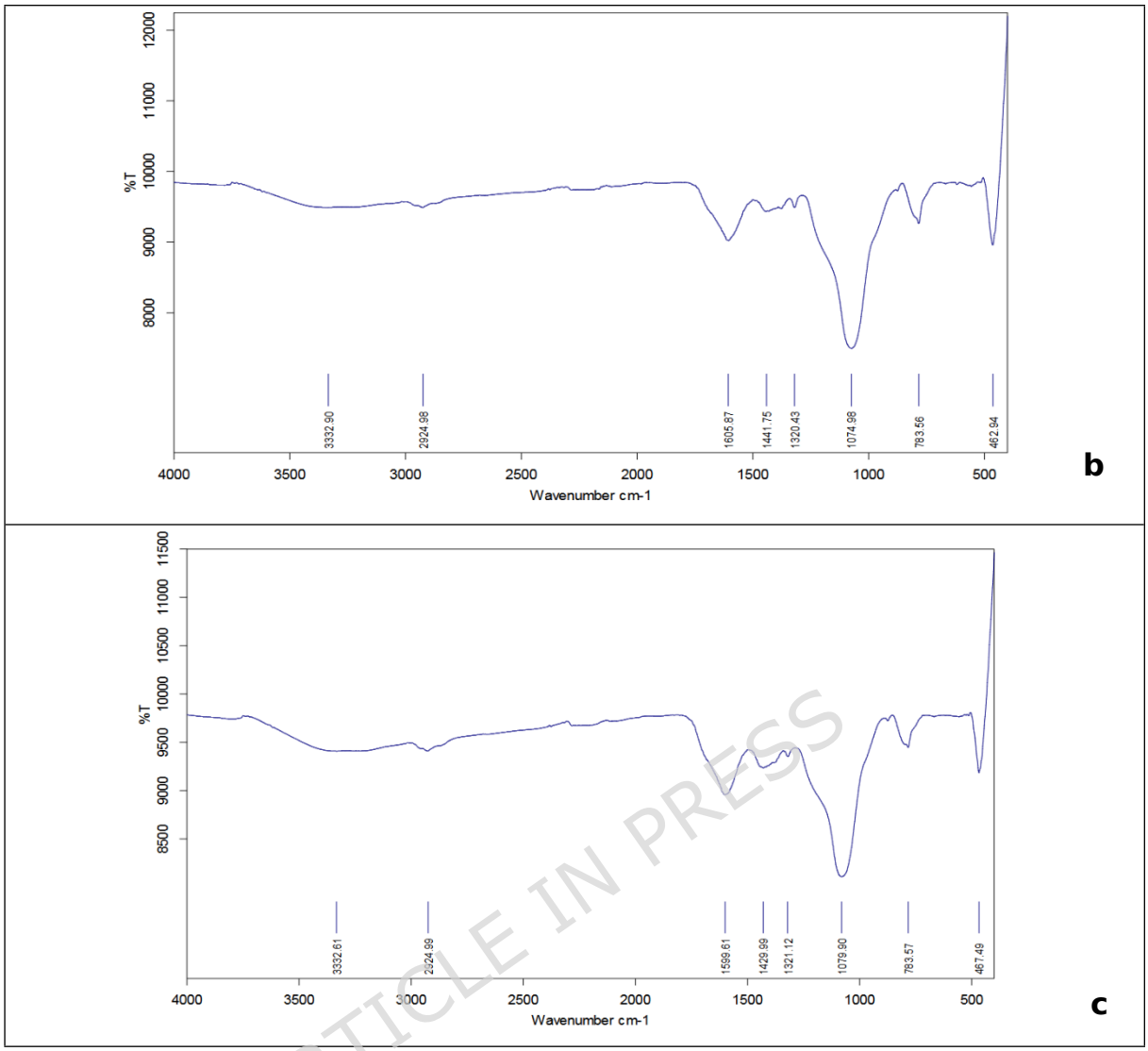

Figure 1. FT-IR spectra of the biochar obtained from pyrolysis of corn stalk(a), rice husk (b), and their 1:1 (w/w) mixture (c) (Values are presented as mean ± standard deviation, n = 3)

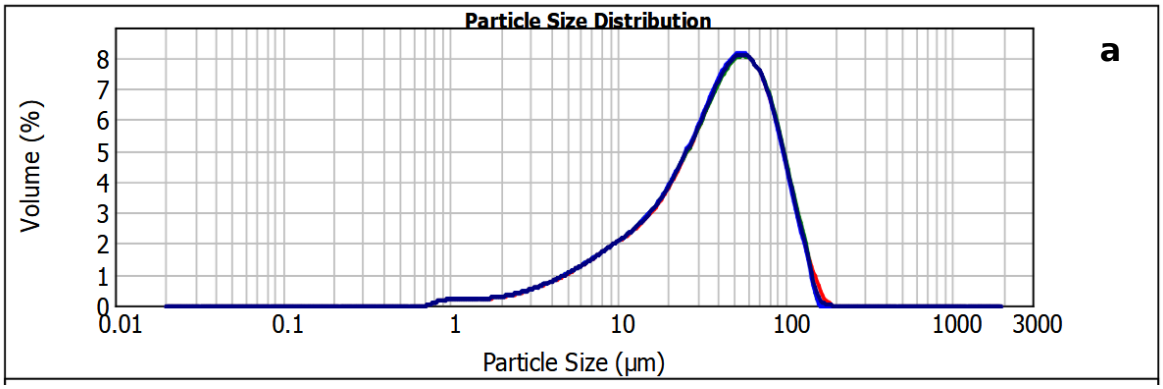

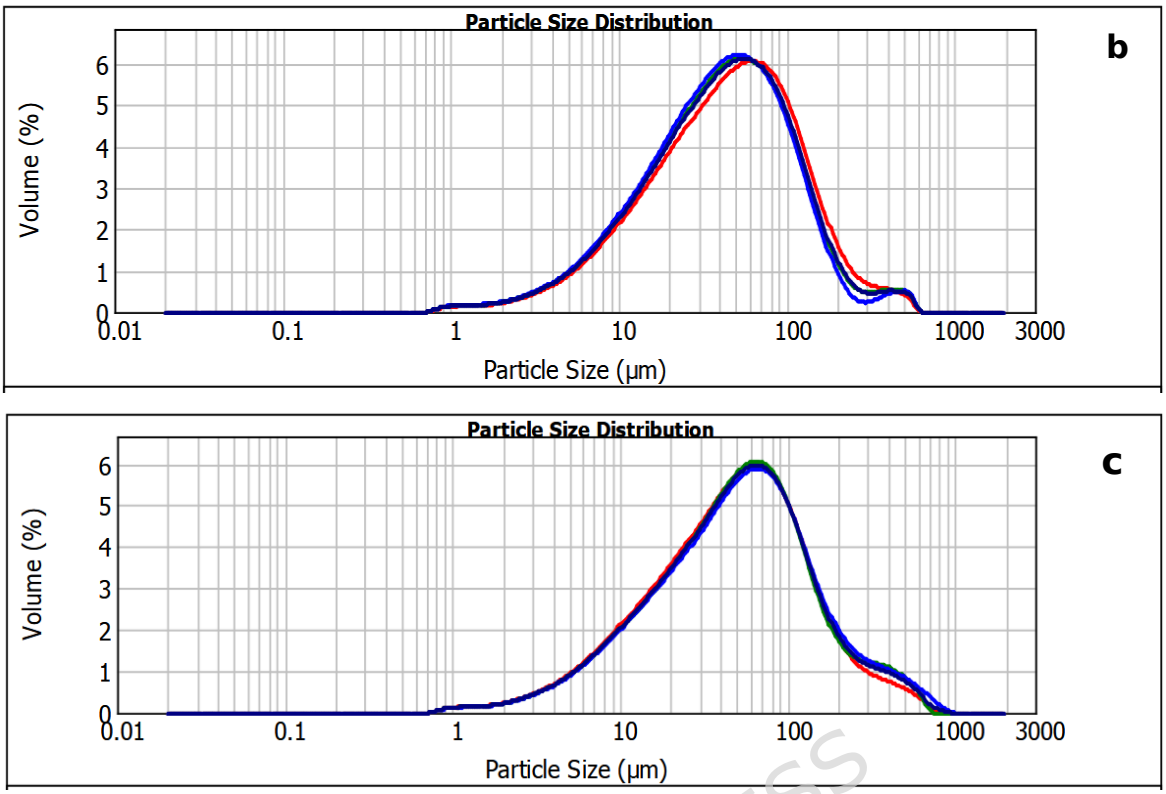

Figure 2. Particle size distribution analysis of the biochar obtained from pyrolysis of corn stalk (a), rice husk (b), and their 1:1 (w/w) mixture (c). *Each curve represents replicate measurements, and the results are presented as mean ± standard deviation (n = 3), demonstrating the reproducibility of the particle size distributions.*

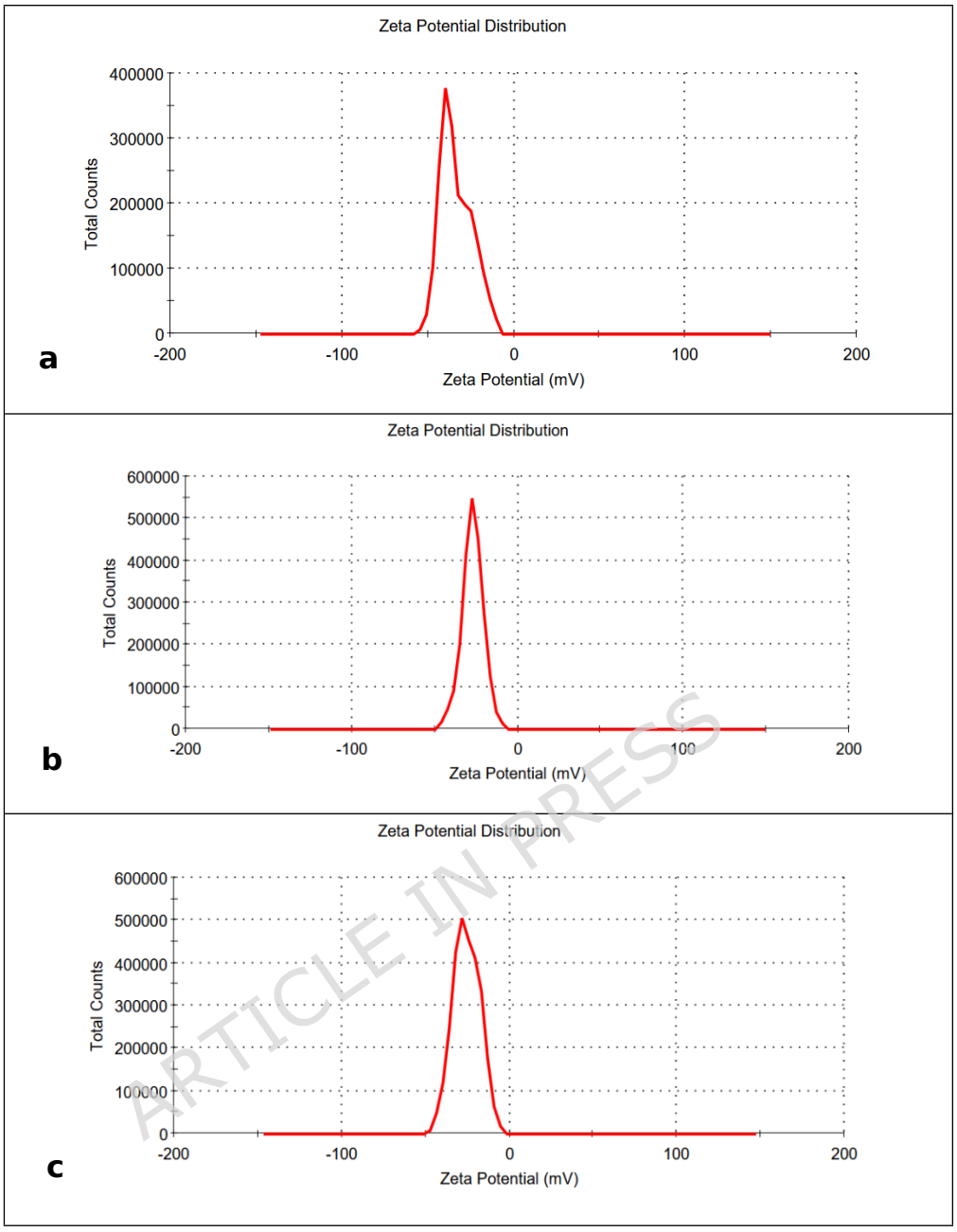

Figure 3. Zeta potential of the biochar obtained from pyrolysis of corn stalk(a), rice husk (b),
and their 1:1 (w/w) mixture (c) (Values are presented as mean ± standard deviation, n = 3)

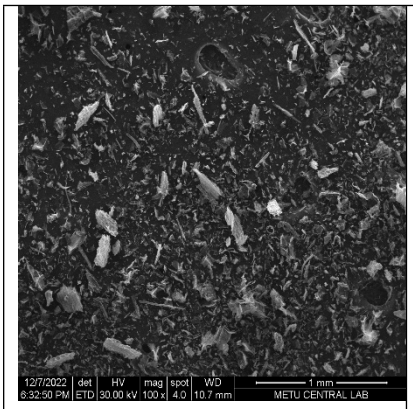

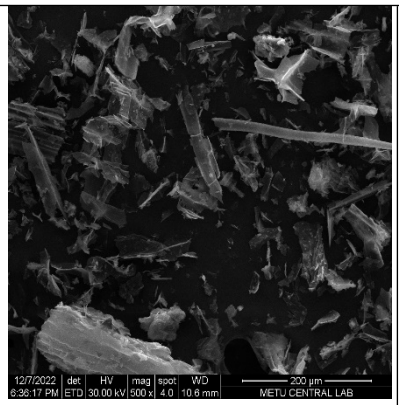

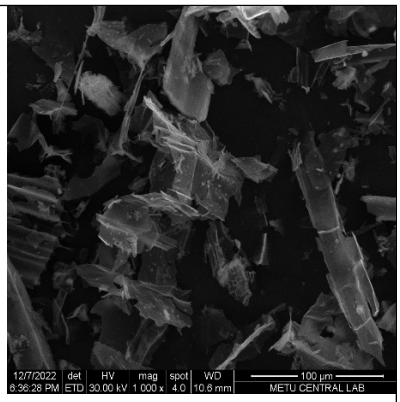

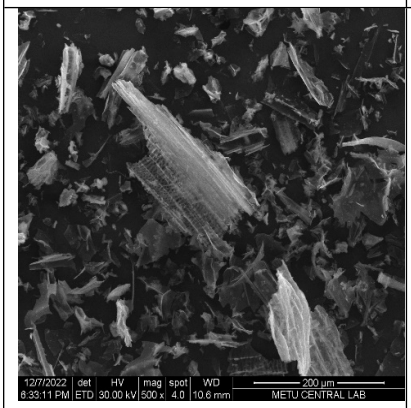

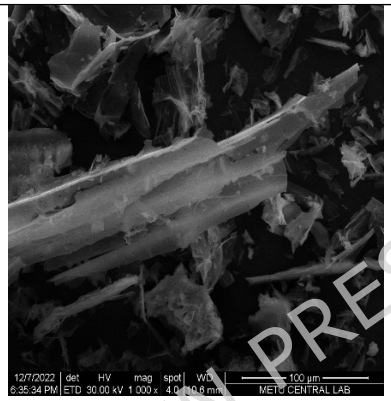

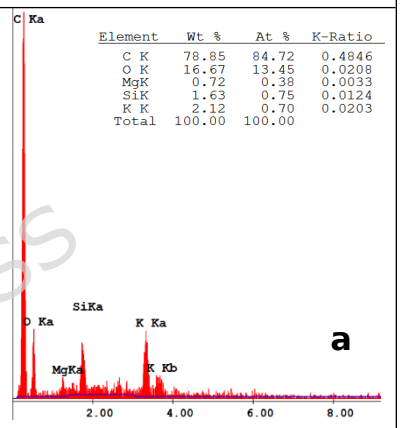

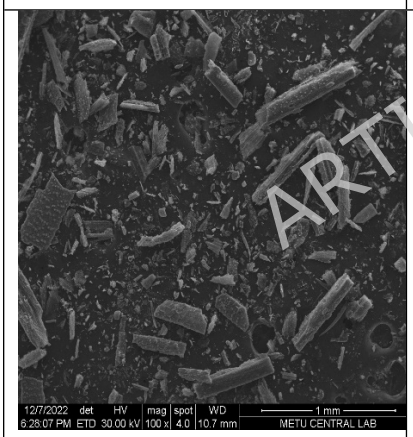

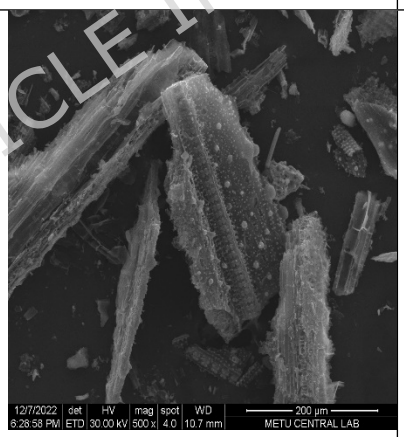

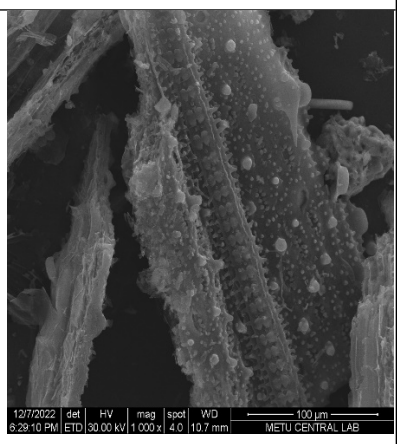

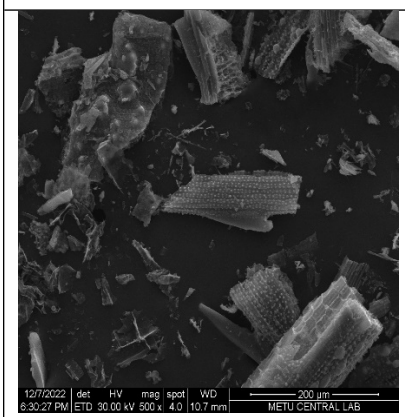

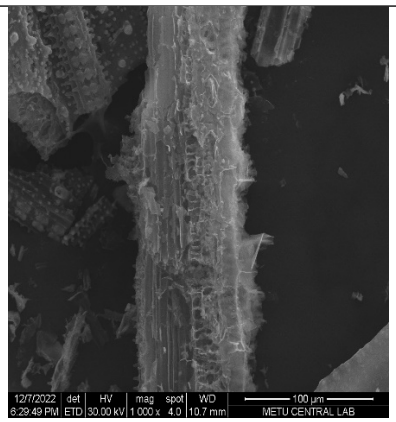

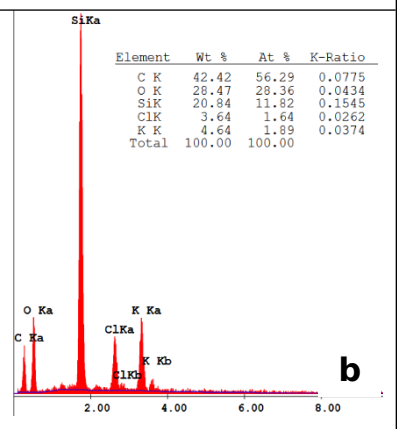

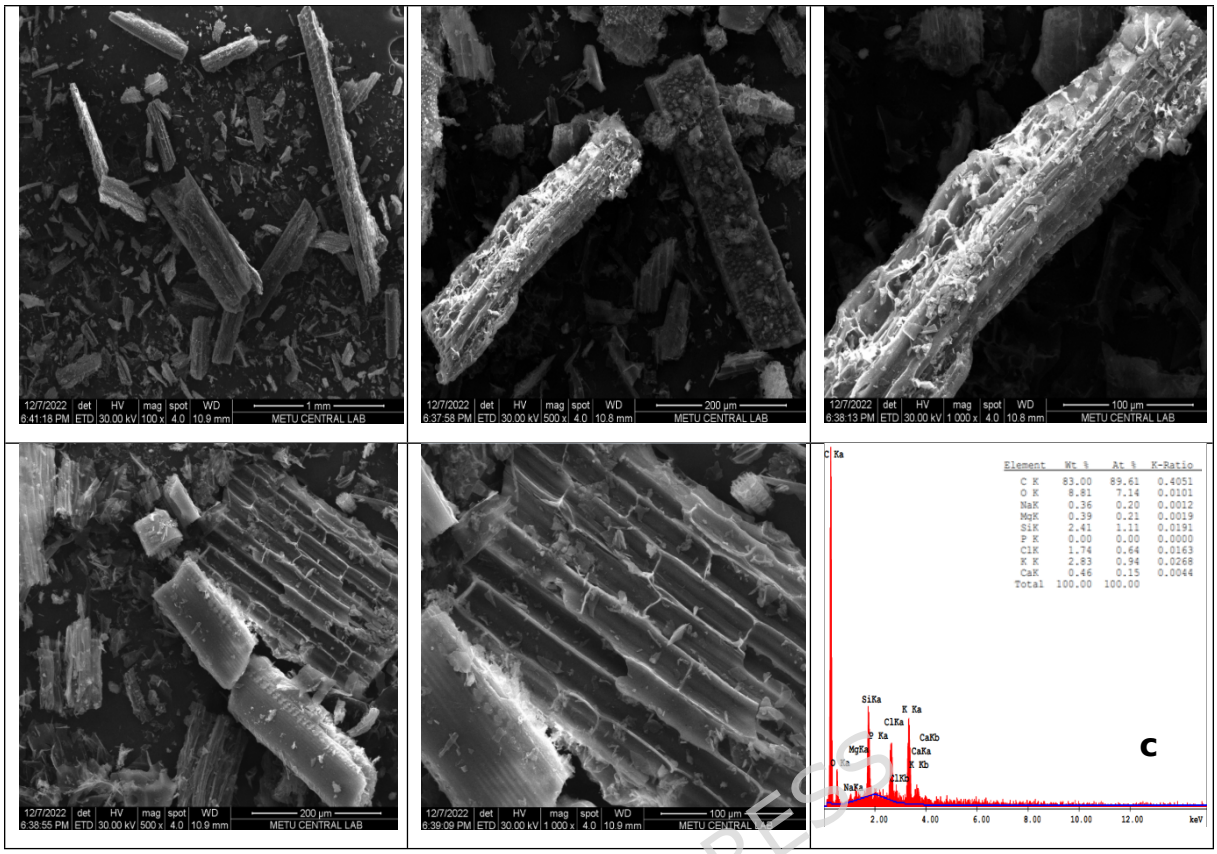

Figure 4. SEM images and EDX analyses of the biochar obtained from pyrolysis of corn stalk(a), rice husk (b), and their 1:1 (w/w) mixture (c). EDX elemental compositions were obtained from three independent measurement points and reported as average values (n = 3).

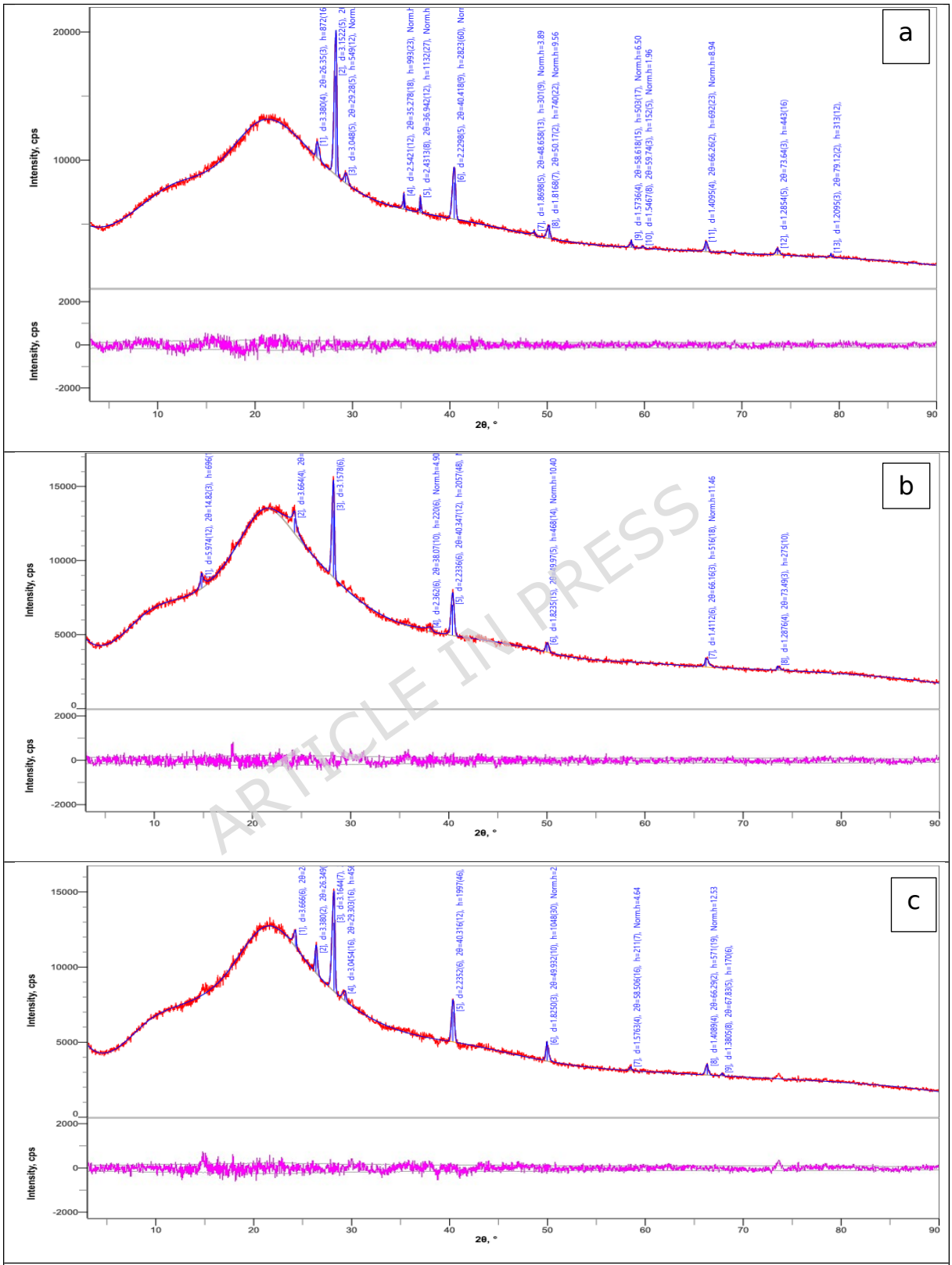

Figure 5. XRD analyses of the biochar obtained from pyrolysis of corn stalk(a), rice husk (b), and their 1:1 (w/w) mixture (c) (Values are presented as mean ± standard deviation, n = 3)

Table 1. Element and compound (oxide form) content of the biochar samples determined by XRF analysis (Values are presented as mean ± standard deviation, n = 3)

Corn stalk-derived biochar				Rice husk- derived biochar				1:1 (w/w) mixture			
comp.	wt%	comp.	wt%	comp.	wt%	comp.	wt%	comp.	wt%	comp.	wt%
Si	12.10 ± 0.35	SiO_2	21.00 ± 0.45	Si	43.70 ± 0.75	SiO_2	63.70 ± 0.90	Si	31.30 ± 0.06	SiO_2	47.80 ± 0.80
K	38.30 ± 0.70	K_2O	32.30 ± 0.60	K	27.20 ± 0.55	K_2O	16.40 ± 0.40	K	24.90 ± 0.05	K_2O	17.30 ± 0.40
Ca	23.20 ± 0.50	CaO	21.00 ± 0.45	Ca	13.70 ± 0.35	CaO	8.52 ± 0.25	Ca	18.80 ± 0.45	CaO	13.90 ± 0.35
Fe	9.79 ± 0 20	Fe_2O_3	8.59 ± 0.18	Fe	1.01 ± 0.03	Fe_2O_3	0.60 ± 0.02	Fe	9.32 ± 0.20	Fe_2O_3	6.47 ± 0.15
Cl	9.81 ± 0.22	Cl	7.39 ± 0.18	Cl	8.23 ± 0.20	Cl	4.49 ± 0.12	Cl	8.02 ± 0.18	Cl	4.98 ± 0.13
Al	1.36 ± 0.04	Al_2O_3	2.11 ± 0.06	Al	0.14 ± 0.01	Al_2O_3	0.20 ± 0.01	Al	2.33 ± 0.06	Al_2O_3	3.29 ± 0.08
Mg	2.21 ± 0.06	MgO	3.07 ± 0.08	Mg	1.13 ± 0.03	MgO	1.42 ± 0.04	Mg	1.47 ± 0.04	MgO	1.88 ± 0.05
S	0.87 ± 0.02	SO_3	1.66 ± 0.04	S	1.36 ± 0.04	SO_3	1.90 ± 0.05	S	0.94 ± 0.03	SO_3	1.49 ± 0.04

Mn	0.44 ± 0.02	P_2O_5	1.46 ± 0.04	Mn	1.99 ± 0.05	P_2O_5	0.81 ± 0.03	Mn	0.81 ± 0.03	P_2O_5	1.05 ± 0.03
P	0.82 ± 0.03	Na_2O	-	P	0.62 ± 0.02	Na_2O	0.78 ± 0.02	P	0.72 ± 0.02	Na_2O	0.56 ± 0.02
Ti	0.71 ± 0.02	TiO_2	0.74 ± 0.02	Ti	-	TiO_2	-	Ti	0.67 ± 0.02	TiO_2	0.56 ± 0.02
Na	-	MnO	0.35 ± 0.01	Na	0.66 ± 0.02	MnO	1.07 ± 0.03	Na	0.45 ± 0.02	MnO	0.51 ± 0.02
Sr	0.16 ± 0.01	SrO	0.12 ± 0.01	Sr	0.10 ± 0.01	SrO	0.05 ± 0.01	Sr	0.20 ± 0.01	SrO	0.11 ± 0.01
Zn	0.23 ± 0.01	ZnO	0.17 ± 0.01	Zn	0.09 ± 0.01	ZnO	0.04 ± 0.01	Zn	0.12 ± 0.01	ZnO	0.07 ± 0.01

Values are presented as mean ± standard deviation (n = 3).

The 1:1 (w/w) mixture biochar was produced from an equal mass mixture of corn stalk and rice husk via co-pyrolysis at 400 °C under oxygen-limited conditions.

Table 2. Comparative particle size analysis of the biochar samples (Values are presented as mean ± standard deviation, n = 3)

Sample	Volume-weighted mean diameter (μm)	Surface-weighted mean diameter (μm)	d(0.1)* (μm)	d(0.5)* (μm)	d(0.9)* (μm)	SPAN value*
Corn stalk-derived biochar	46.47 ± 2.15	17.95 ± 0.82	8.75 ± 0.28	40.79 ± 1.76	92.59 ± 4.12	2.06 ± 0.09
Rice husk-derived biochar	63.16 ± 2.84	19.62 ± 0.91	9.35 ± 0.31	42.39 ± 1.98	131.84 ± 5.37	2.89 ± 0.12
1:1 (w/w) mixture biochar	80.75 ± 3.52	21.13 ± 1.04	9.67 ± 0.34	49.61 ± 2.15	176.48 ± 7.21	3.36 ± 0.14

*d(0.1), d(0.5), and d(0.9) represent the particle diameters at 10%, 50%, and 90% of the cumulative volume distribution, respectively.

SPAN represents the width of the particle size distribution. Values are expressed as mean ± standard deviation (n = 3), indicating experimental variability and allowing quantitative comparison among samples.

The 1:1 (w/w) mixture biochar was produced from an equal mass mixture of corn stalk and rice husk via co-pyrolysis at 400 °C under oxygen-limited conditions.

Table 3. Comparative physicochemical properties of biochars derived from corn stalk, rice husk, and their 1:1 (w/w) mixture (Values are presented as mean ± standard deviation, n = 3)

Analyses	Corn stalk-derived biochar	Rice husk-derived biochar	1:1 (w/w) mixture biochar
Moisture, %	3.29 ± 0.08	3.50 ± 0.07	3.28 ± 0.06
Organic matter, %	75.49 ± 0.62	65.93 ± 0.55	64.87 ± 0.58
pH	7.52 ± 0.05	7.84 ± 0.04	7.69 ± 0.06
Electrical conductivity (dS/m)	4.70 ± 0.12	5.80 ± 0.15	5.62 ± 0.13
Total N, %	0.84 ± 0.04	1.27 ± 0.05	1.32 ± 0.06
Total P_2O_5, %	1.19 ± 0.04	1.23 ± 0.05	1.16 ± 0.04
Total K_2O, %	1.76 ± 0.07	1.68 ± 0.06	1.50 ± 0.05
Toplam SO_3, %	0.28 ± 0.02	0.33 ± 0.02	0.30 ± 0.02

Values are presented as mean ± standard deviation (n = 3).

The 1:1 (w/w) mixture biochar was produced from an equal mass mixture of corn stalk and rice husk via co-pyrolysis at 400 °C under oxygen-limited conditions.